Available online at www.sciencedirect.com
ScienceDirect
Journal of Molecular Catalysis A: Chemical 271 (2007) 32–41
JOURNAL OF MOLECULAR CATALYSIS A: CHEMICAL
www.elsevier.com/locate/molcata

Formation of nitroxide radicals from secondary amines and peracids: A peroxyl radical oxidation pathway derived from electron spin resonance detection and density functional theory calculation

Hong-Chang Shi *, Yong Li

Department of Chemistry, Tsinghua University, Beijing 100084, China

Received 23 September 2006; received in revised form 3 February 2007; accepted 6 February 2007
Available online 17 February 2007

Abstract

By electron spin resonance (ESR) detection and quantum chemical calculation based on the density functional theory (DFT) at the B3LYP/6-31G(d) level, we found that the formation of nitroxide radicals from secondary amines and peracids is a peroxyl radical oxidation reaction, where peroxyl radicals are the reactive intermediates of peracids in the oxidation. The DFT calculation revealed the transition structures and activation barriers of oxidizing pyrrolidine by the peroxyl radicals of peracetic acid and percarboximidic acid. Their barriers are 11.75 and 12.35 kcal/mol, respectively, showing that the peroxyl radicals have high reactivity on secondary amines. A reaction path calculation (IRC) of the oxidation of pyrrolidine by the peroxyl radical of percarboximidic acid illustrated the process of the formation of nitroxide radical: firstly, the terminal oxygen atom of the peroxyl radical R–O–O• attacks the nitrogen atom of secondary amine and forms a N–O bond, and then the hydrogen atom from the N–H of the secondary amine is transferred to the imido nitrogen atom or the carbonyl oxygen atom of peracid and finally forms a new N–H or O–H bond.

Keywords: Secondary amine; Peroxyl radical; Nitroxide radical; ESR detection; DFT calculation

1. Introduction

Stable nitroxide radicals as spin labels and spin probes play important roles in the study of biological systems using electron spin resonance (ESR) spectroscopy. Since the 1960s, a large number of experimental and theoretical research projects have been carried out to investigate the synthesis, structure, properties and application of nitroxides [1–21]. Preparation of nitroxide radicals through oxidization of secondary amines by peracids has been the most important synthesis method and has been extensively investigated. Among peracids, *m*-chloroperbenzoic acid (MCPBA) is the most effective and most widely used oxidant [8–18]. Peracetic acid is also used sometimes [19–21].

The acetonitrile-hydrogen peroxide method of Payne et al. [22] is another useful procedure for preparing nitroxide radicals. For example, the ester secondary amine was oxidized at room temperature to a nitroxide radical with a yield of 88% as shown below [23]. However, this actually can also be ascribed to the method of using peracids because in the reaction the acetonitrile would first be changed into percarboximidic acid as mentioned later.

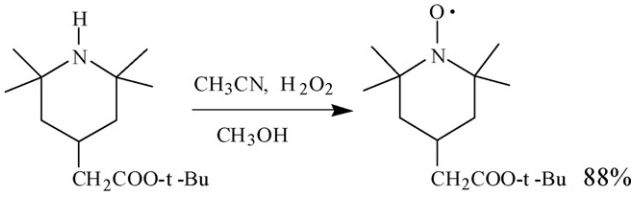

Throughout the last 40 years, although many nitroxide radicals have been synthesized, the mechanism of their formation remains unclear. To date, it is still not understood how secondary amines change into nitroxide radicals. The questions are what the reactive intermediate of the reaction is, what the transition structure is, how high the activation barrier of the oxidation reaction is, how the unpaired electron of nitroxide is produced and how the relative atoms are transferred.

By a quantum chemical calculation with the density functional theory (DFT) at the B3LYP/6-31G(d) level, it was found

* Corresponding author. Tel.: +86 10 62783878; fax: +86 10 62771149.
E-mail address: shihc@mail.tsinghua.edu.cn (H.-C. Shi).

1381-1169/$ – see front matter © 2007 Elsevier B.V. All rights reserved.
doi:10.1016/j.molcata.2007.02.012

that the formation of the nitroxide radicals is a radical oxidation reaction of secondary amines by peroxyl radicals. The peroxyl radicals are the products from peracid molecules missing the H atoms in the −OOH groups. The transition structures (**TS**) and the activation barriers of oxidizing pyrrolidine by the peroxyl radicals $CH_3C(O)OO^{\bullet}$ and $CH_3C(NH)OO^{\bullet}$ were obtained. The barriers were low; only ∼10 kcal/mol. ESR detection also indicated that the activation barriers in the formation of nitroxide radicals are fairly low. A reaction path calculation (IRC) revealed the microscopic process of forming nitroxide radicals.

2. Experimental

All the chemical reagents were commercial guaranteed reagents, and were used without any further purification. The samples used for ESR measurements were prepared by adding pyrrolidine or dimethylamine and 30% of H_2O_2 into CH_3CN–H_2O (v/v, 20:80). The concentration of pyrrolidine or dimethylamine was about 0.3 M, and the concentration of H_2O_2 was about 1.0 M. The pH values of the solution were 9.0–10.0 because the secondary amines were basic. In the preparation, it was observed that some O_2 bubbles were released. All ESR spectra were recorded at room temperature using a Bruker ER-200D spectrometer.

3. Quantum chemical calculations

The DFT calculation was carried out with the Gaussian 98 program package [24]. In the last decade, the DFT method has become an important tool in clarifying reaction mechanism, especially for some difficult controversial mechanistic problems [25–31]. Recently, Schiemann and co-workers [8] used the DFT method to calculate the electric structures of some aromatic nitroxide radicals, obtaining result that is in very good agreement with the experimental data. Therefore, in the present study we selected the DFT method to explore the mechanism of the formation of nitroxide radicals from secondary amines and peracids. Geometry optimizations of radical or non-radical

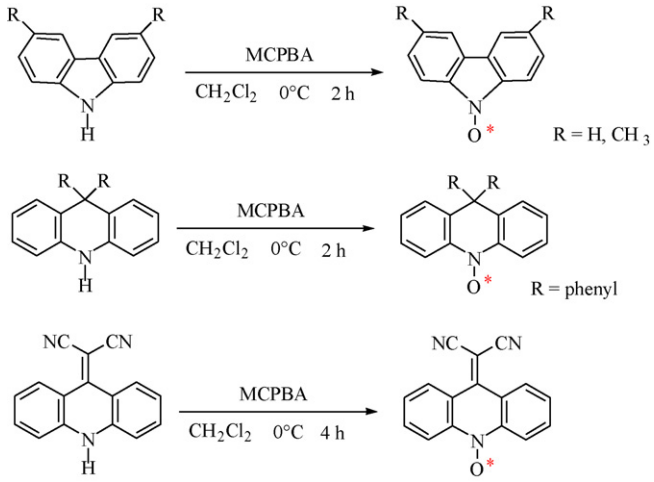

Scheme 1. The nitroxide radicals generated at 0 °C.

Table 1
ESR spectral parameters of the radicals **5** and **3**

Radical	g_{iso}	**a**(N) (mT)	No. of nitrogen	**a**(H_β) (mT)	No. of proton
I	2.0069	1.51	1	1.96	4
II	2.0060	1.59	1	1.08	4

molecules, the geometries of transition structures, potential energy surface scans (PES), reaction path calculation (IRC), and estimation of solvent effects by using the polarizable continuum model (PCM) (32–35) were all carried out at the B3LYP/6-31G(d) level. Obviously, using the same calculation method, level and basis set is favorable for comparing the data and achieving reliable conclusion.

4. Results and discussion

4.1. Formation of nitroxide radicals is a reaction process with low activity barriers

The oxidation of secondary amines by peracids often occurs at temperature between 0 and 25 °C. Recently, Schiemann and

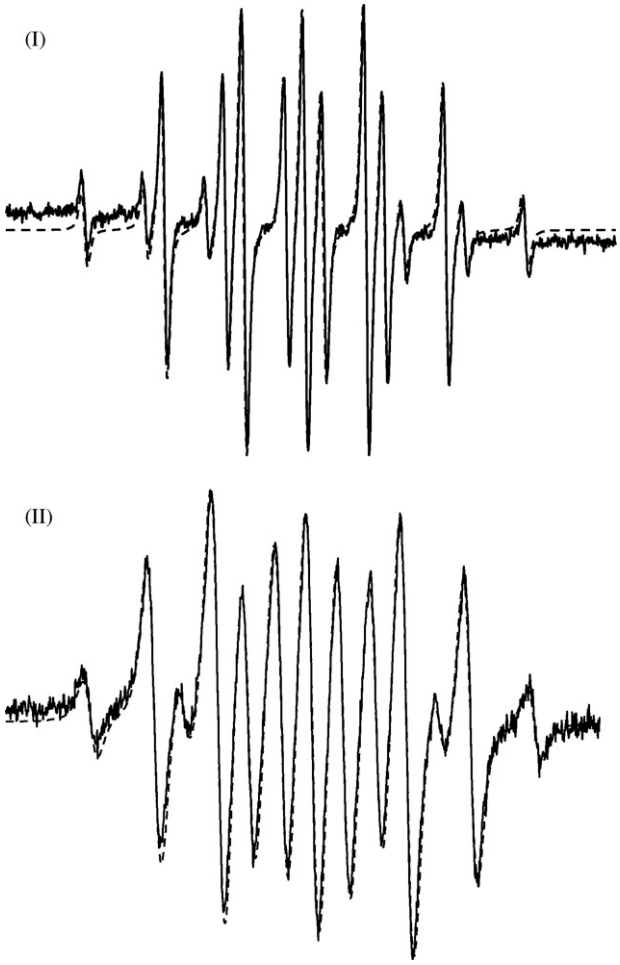

Fig. 1. Experimental (solid line) and computer simulated (dashed line) ESR spectra of pyrrolidine—N—oxide radical (I) and dimethylamine—N—oxide radical (II) at room temperature.

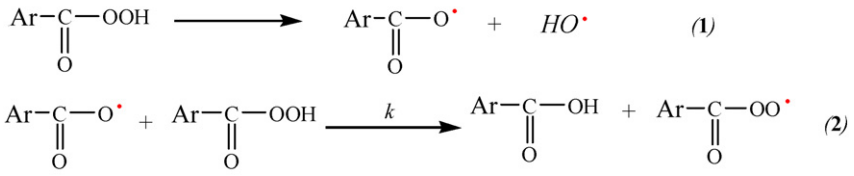

Scheme 2. Homolysis of the peroxy bond of aromatic peracids and formation of acylperoxyl radical.

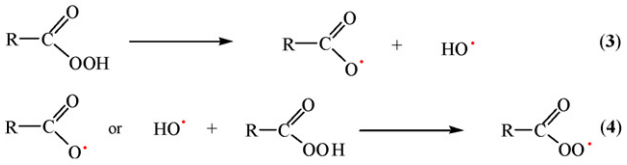

Scheme 3. Homolysis of the peroxy bond of peracids and formation of acylperoxyl radical.

co-workers [8] used MCPBA to oxidize some aromatic secondary amine compounds at 0 °C and successfully obtained their stable nitroxide radicals (Scheme 1).

Most stable nitroxide radicals are synthesized from the secondary amine in which there are no hydrogen atoms attached to α-carbon atoms. When the α-carbon atom of a nitroxide radical has one or several hydrogen atoms, the radical is quite unstable [36]. In the present study, we used the acetonitrile-hydrogen peroxide method for oxidizing pyrrolidine and diethylamine at room temperature (20 °C). For the two secondary amines with four α-hydrogen atoms their nitroxide radicals were certainly unstable, but ESR measurements (Fig. 1 (**I** and **II**)) showed that using this method they both can be easily changed into nitroxide radicals. This indicated that significant amounts of the two nitroxide radicals could be generated at room temperature and their lifetimes were long enough to be observed by ESR.

As indicated by the solid lines in Fig. 1, the spectra contain a triplet with the same intensities and each triplet line is further split into a quintet with intensities of 1:4:6:4:1. This is easily explained: the triplet peaks that arose from the hyperfine splitting were due to one nitrogen atom of the radical generated in the system with a hyperfine coupling constant (hfcc, **a**(N)) and the quintet was due to four identical β-protons with $\mathbf{a}(H_\beta)$. The ESR parameters are summarized in Table 1. The experimental ESR spectra were well simulated using the WINEPR Simfonia program (Fig. 1, dashed line) based on the ESR parameters in Table 1. The ESR lineshapes and parameters were typical of nitroxide radicals. This means that the two ESR spectra were due to the nitroxide radicals of pyrrolidine and diethylamine.

These results confirmed that the activation barriers of nitroxide radical formation are fairly low. This conclusion from the experiments is consistent with the following results obtained by DFT calculation.

4.2. Generation of peroxyl radicals

In the DFT calculation at the B3LYP/6-31G(d) level, we tried using many peroxyl compounds to oxidize pyrrolidine, such as neutral HOOH, $CH_3C(O)OOH$, $CH_3C(NH)OOH$, and their negative ions HOO^-, $CH_3C(O)OO^-$, and $CH_3C(NH)OO^-$, but did not find any oxidation reactivity to generate the nitroxide radicals of pyrrolidine. Only peroxyl radicals R–C(O)OO• and R–C(NH)OO• showed oxidation reactivity on secondary amines and the reactivity was fairly high.

Many researchers [37–41] have already proven that the oxidation of alkanes by aromatic peracids proceeds through a radical mechanism. The mechanism involves the homolysis of the peroxy bond of peracids (Scheme 2(**1**)) and abstraction of hydrogen from the –OOH group of peracids by an acyloxyl radical to produce the acylperoxyl radical (Scheme 2(**2**)). Reaction 2 is fairly rapid, and the rate constant k has been found [42,43] to be in the range of 10^5–10^6 M^{-1} s^{-1}.

The radical reactions in Scheme 2 also should be suitable for non-aromatic peracids (Scheme 3(**3** and **4**)), because they have identical peroxyl groups. The difference between aromatic and non-aromatic peracids is only that the aromatic rings of aromatic peracids can increase the stability of their radicals, and so they probably have stronger oxidation activity than non-aromatic peracids.

For acetonitrile-hydrogen peroxide systems a similar reactive peroxyl radical can be produced. Wiberg [44–46] established the reaction mechanism of nitriles with H_2O_2 (Scheme 4), according to which, under weak basic conditions, nitriles were first oxidized by hydrogen peroxide to percarboximidic acid (Scheme 4(**5**)) and then could be changed into amide and O_2 (Scheme 4(**6**)).

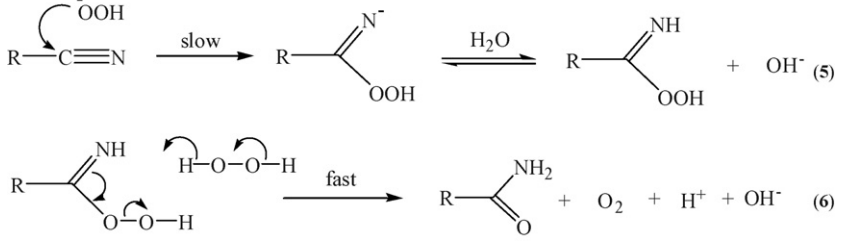

Scheme 4. Wiberg's reaction mechanism of nitriles with hydrogen peroxide and formation of percarboximidic acid.

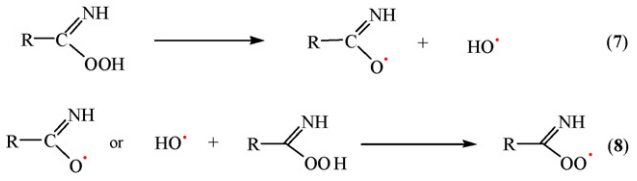

Scheme 5. Formation of the peroxyl radical of percarboximidic acid.

The percarboximidic acid is also a peracid and so can carry out the hydrogen abstraction reaction to form peroxyl radicals, as shown in Scheme 5, similar to Schemes 2 and 3. Therefore, for the oxidation of secondary amine in the acetonitrile-hydrogen peroxide systems, the reactive oxidant can be considered to be the peroxyl radical of percarboximidic acid.

The calculation at the B3LYP/6-31G(d) level indicated that in the hydrogen abstraction reaction from the –OOH group of peracids the energies of all of the reaction systems decreased significantly (Scheme 6).

By DFT calculation at the B3LYP/6-31G(d) level, we obtained the transition structures **TS1**–**TS4** and activation barriers of the hydrogen abstractions of $CH_3C(O)OOH + HO^{\bullet}$ (1) or $+CH_3C(O)O^{\bullet}$ (2); $CH_3C(NH)OOH + HO^{\bullet}$ (3) or $+CH_3C(NH)O^{\bullet}$ (4) The transition structures are shown in Fig. 2 (the initial structures are omitted). The activation barriers were calculated based on the energies and zero point energy (ZPE) correction of the systems, which are shown in Table 2.

From the data in Table 2, the activation barriers (ΔE^{*}) of the hydrogen abstraction are extremely low, even negative and all are negligible. Therefore, if the peroxy bond of peracids is homolytically cleaved into two radicals, the radicals would easily convert peracid molecules into corresponding peroxyl radicals. This may be why the formation of the peroxyl radicals is very rapid ($k = 10^5$–$10^6\ M^{-1}\ s^{-1}$).

According to Table 2, $CH_3C(NH)O^{\bullet}$ have high reactivity in the production of peroxyl radicals, because its activation barrier for hydrogen abstraction is extremely low. By using acetonitrile-hydrogen peroxide method of Payne et al. [22] we easily obtained the ESR spectra of the nitroxide radicals (Fig. 1) of pyrrolidine and diethylamine at room temperature. A logical reason is that the systems easily generate the peroxyl radical of percarboximidic acid.

4.3. Formation of clusters: a spontaneous transfer of the lone-pair electrons on the N atom of secondary amine toward the peroxyl radical

By DFT calculation at the B3LYP/6-31G(d) level we found that secondary amines and peroxyl radicals can spontaneously form unusual clusters.

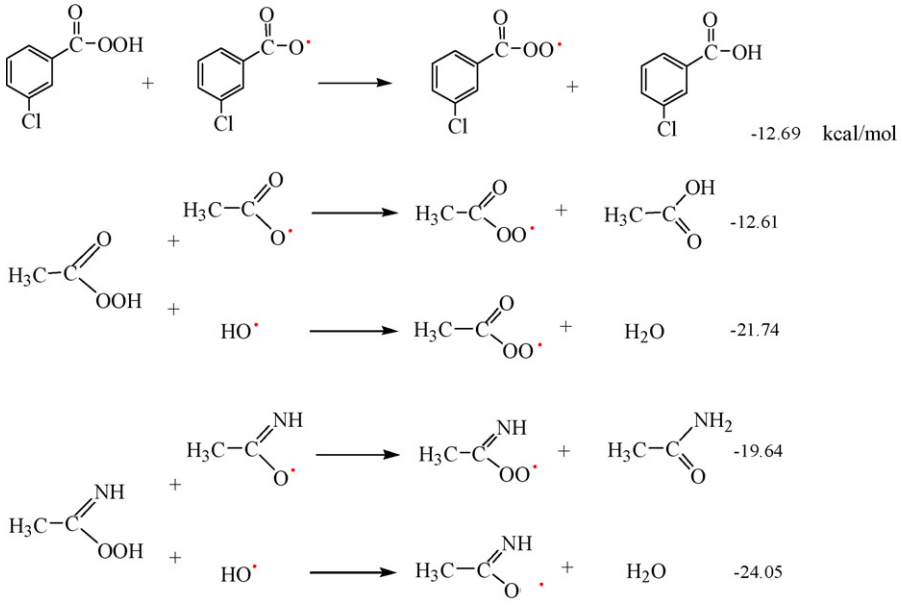

Scheme 6. The hydrogen abstraction from the –OOH group of peracids produced the peroxyl radicals and the energies of the systems were remarkably lower by DFT calculation at the B3LYP/6-31G(d) level.

Table 2
Activation barriers (ΔE^{*}) obtained from electronic energies (E_{TS}, $E_{initial}$), zero-point correction energies (ZPE_{TS}, $ZPE_{initial}$) of initial and transition structures (**TS**) of $CH_3C(O)OOH + HO^{\bullet}$ (1), $CH_3C(\mathbf{1})OOH + CH_3C(O)O^{\bullet}$ (**2**), $CH_3C(NH)OOH + HO^{\bullet}$ (**3**) and $CH_3C(NH)OOH + CH_3C(NH)O^{\bullet}$ (**4**)

	E_{TS} (a.u.)	ZPE_{TS} (a.u.)	$E_{initial}$ (a.u.)	$ZPE_{initial}$ (a.u.)	Radical	ΔE^{*} (kcal/mol)
1	−379.939089	0.071977	−379.946273	0.076810	$HO^{\bullet}$	4.51 (1.48)
2	−532.616171	0.109222	−532.627203	0.114345	$CH_3C(O)O^{\bullet}$	6.92 (3.71)
3	−360.048698	0.084405	−360.059065	0.089707	$HO^{\bullet}$	6.50 (3.18)
4	−492.849149	0.136169	−492.849805	0.139650	$CH_3C(NH)O^{\bullet}$	0.41 (−1.77)

The data in parentheses are with the zero-point correction energies.

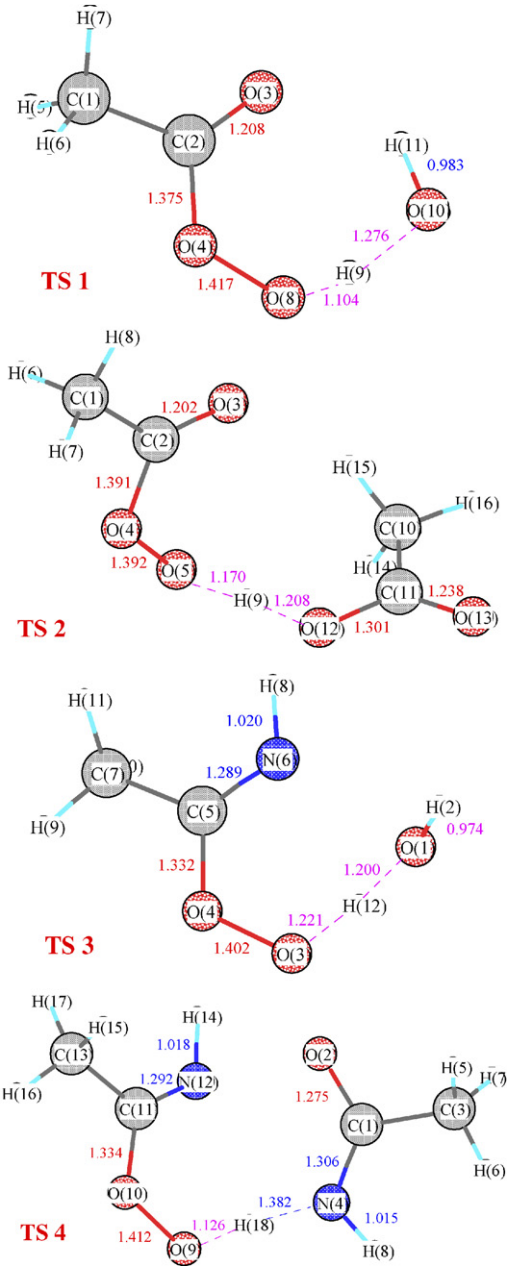

Fig. 2. Transition structures TS1–TS4 of the hydrogen abstractions of $CH_3C(O)OOH + HO^{\bullet}$ (**1**) or $+CH_3C(O)O^{\bullet}$ (**2**); $CH_3C(NH)OOH + HO^{\bullet}$ (**3**) or $+CH_3C(NH)O^{\bullet}$ (**4**) obtained by DFT calculation at the B3LYP/6-31G(d) level.

For reaction systems of pyrrolidine and $CH_3C(O)OO^{\bullet}$ or $CH_3C(NH)OO^{\bullet}$ peroxyl radicals, when the distance between N(3) and O(15) is greater than 4.9 or 3.9 Å (Fig. 3($\mathbf{a}_1$ and $\mathbf{b}_1$)), no electron transfer occurs between pyrrolidine and the peroxyl radical. The graphs $\mathbf{a}_1$ and $\mathbf{b}_1$ show that the highest spin density of the unpaired electron is on the end oxygen atom of the peroxyl radical. The second highest is on another oxygen atom of the peroxy bond, and the rest are on the carbonyl oxygen atom or on the nitrogen atom of the imido group. When the distance is close to 4.70 or 3.81 Å (Fig. 3($\mathbf{a}_2$ and $\mathbf{b}_2$)), respectively, the electron transfer starts. Then the N atom of pyrrolidine carries a small unpaired electron population. The distance of 4.70 or 3.81 Å between the end oxygen atom of the peroxyl radical and the N atom of pyrrolidine is too far for the electron transfer. The electron transfer may take place through O(18)···H(10) or N(18)···H(10) because the distances (2.14 or 2.17 Å) are much shorter than those between N(3) and O(15).

When the distances between N(3) and O(15) are 2.265 or 2.343, clusters of pyrrolidine and the corresponding peroxyl radicals are formed. The spin density surface graph of $\mathbf{a}_{cluster}$ is shown in Fig. 4 (the graph for $\mathbf{b}_{cluster}$ is shown in Fig. 7). A potential energy surface (PES) scan calculation from $\mathbf{a}_1$ or $\mathbf{b}_1$ to $\mathbf{a}_{cluster}$ or $\mathbf{b}_{cluster}$ shows that this is a spontaneous process because the activation barrier has not appeared. Formation of $\mathbf{a}_{cluster}$ or $\mathbf{b}_{cluster}$ makes the system energy fall to ~10 kcal/mol lower than $\mathbf{a}_1$ or $\mathbf{b}_1$ (Table 3).

It is interesting that the clusters formed by the secondary amine and peroxyl radicals are different from those of non-radical molecules. It is not a simple adduct of the two molecules. In the clusters, approximately half of the unpaired electron population is located on the N atom of pyrrolidine, which indicates that the electron transfer between the secondary amine and peroxyl radicals occurs spontaneously.

The orientation of electron transfer is a problem that must be resolved. According to the calculation, the total Mulliken charges on the peroxyl radicals $CH_3C(O)OO^{\bullet}$ and $CH_3C(NH)OO^{\bullet}$ in $\mathbf{a}_{cluster}$ and $\mathbf{b}_{cluster}$ were −0.28 and −0.25 (Table 3), respectively, and so the transfer evidently is from pyrrolidine to the peroxyl radical. The Mulliken atom spin density on the N(3) atom of pyrrolidine is approximately the same as that of O(15) of the peroxyl radical. This indicated that the lone-pair electron on the N atom of the secondary amine was partly transferred to the peroxyl radical and partly paired with its unpaired electron. This resulted in the N atom of the secondary amine possessing the unpaired electrons.

4.4. The mechanism of generating nitroxide radicals of secondary amines by peracids

By DFT calculation at the B3LYP/6-31G(d) level we have obtained transition structures (Fig. 5) and activation barriers (Table 4) of pyrrolidine oxidation by the peroxyl radicals of peracetic acid and percarboximidic acid. Their activation barriers were low, only ~10 kcal/mol.

Since this is a radical reaction, the reaction system has a singly occupied molecular orbital (SOMO) and the orbital also is the highest occupied molecular orbital (HOMO) of the system. The SOMO graphs and spin density surface graphs of the systems both reflect the unpaired electron population in the systems. Therefore, the two graphs should have similar external form. For example, Fig. 6 shows the SOMO graph and the spin density graph of the transition structure $\mathbf{a}_{TS}$. Obviously, their external forms are approximately the same. From Fig. 6, one can see that at the TS, large unpaired electron populations are still present in pyrrolidine.

The above activation barriers are the result of calculating the bimolecular system of a peroxyl radical and a secondary amine (gas phase). However, the reaction occurs in solvent. Therefore, the influence of the solvent on the activation barrier of the oxidation has to be considered. Solvents CH_2Cl_2, CH_3CN and H_2O

Table 3
The charge and spin density on pyrrolidine and peroxyl radicals in $\mathbf{a}_{cluster}$ and $\mathbf{b}_{cluster}$ and the system energy reduction (ΔE)

	Total charges on the peroxyl radicals	Spin density		$E_{cluster}$ (a.u.)	E_1 (a.u)	ΔE (kcal/mol)
		O(15)	N(3)			
a	−0.28	0.55	0.45	−516.148262	−516.132345	−9.98
b	−0.25	0.55	0.44	−496.257136	−496.240625	−10.36

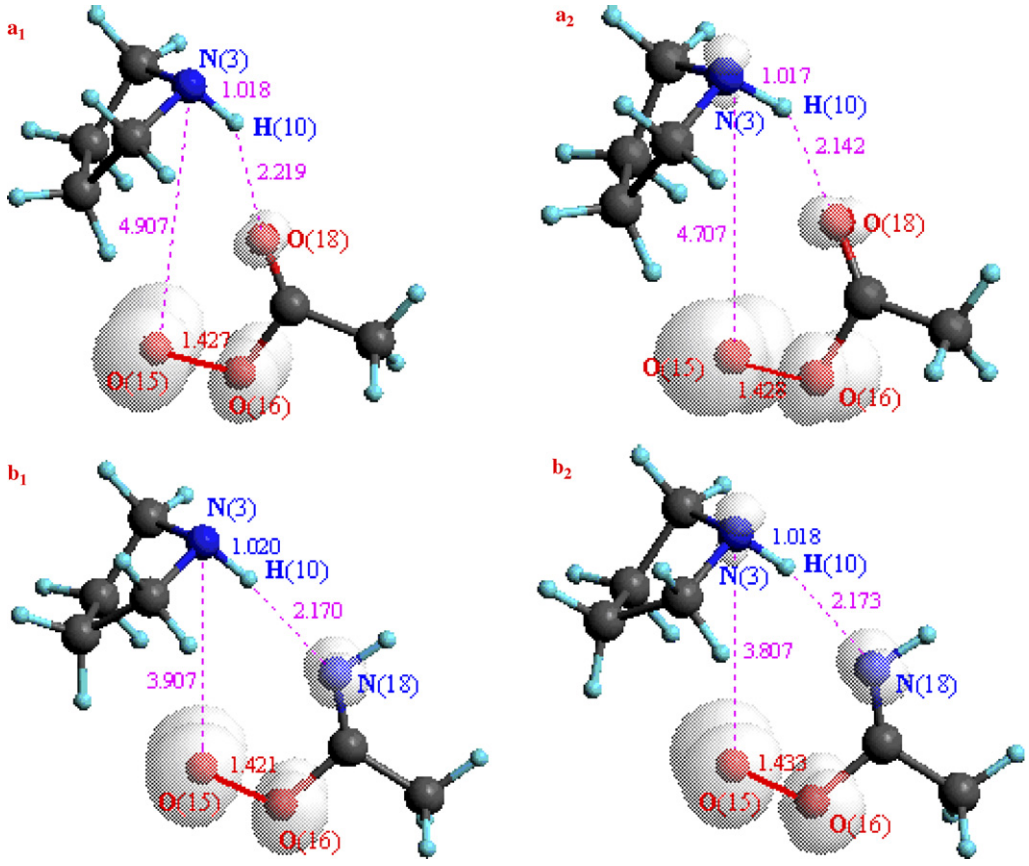

Fig. 3. The spin density surface graphs obtained by DFT calculation at the B3LYP/6-31G(d) level for the systems of pyrrolidine and peroxyl radical $CH_3C(O)OO^{\bullet}$ ($\mathbf{a}_1$, $\mathbf{a}_2$) or $CH_3C(NH)OO^{\bullet}$ ($\mathbf{b}_1$, $\mathbf{b}_2$).

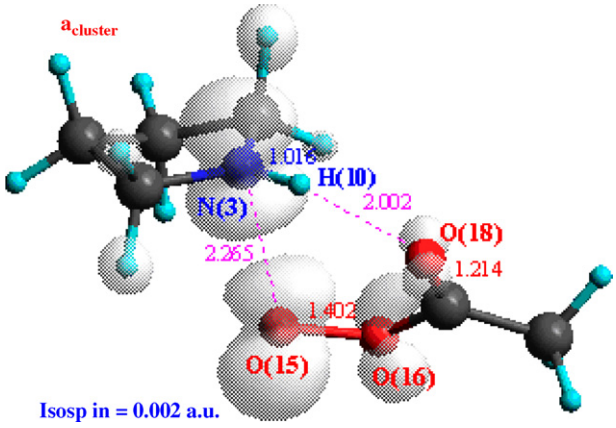

Fig. 4. The spin density surface graph of $\mathbf{a}_{cluster}$ formed by pyrrolidine and the peroxyl radical of peracetic acid obtained by the DFT calculation at the B3LYP/6-31/G(d) level.

were frequently used in the preparation of nitroxide radicals. We used Tomasi's polarized continuum model (PCM) [32–35] to estimate the effects of the solvents. DFT/6-31G(d)/PCM energies E_{TS}, $E_{cluster}$ for CH_2Cl_2, CH_3CN and H_2O were determined by utilizing DFT geometries of the transition structures and the clusters obtained for the bimolecular systems. The calculation results of E_{TS}, $E_{cluster}$ and the activation barriers of including

Table 4
Activation barriers (ΔE^*) obtained based on electronic energies (E_{TS}, $E_{cluster}$), zero-point correction energies (ZPE_{TS}, $ZPE_{cluster}$) of clusters and transition structures (TS) of pyrrolidine and peroxyl radicals of peracetic acid (**a**) or percarboximidic acid (**b**)

	E_{TS}	ZPE_{TS}	$E_{cluster}$	$ZPE_{cluster}$	ΔE^* (kcal/mol)
a	−516.129528	0.184195	−516.148262	0.184270	11.75 (11.70)
b	−496.237442	0.196250	−496.257136	0.196538	12.35 (12.17)

The data in parentheses included zero-point energy correction (ZPE).

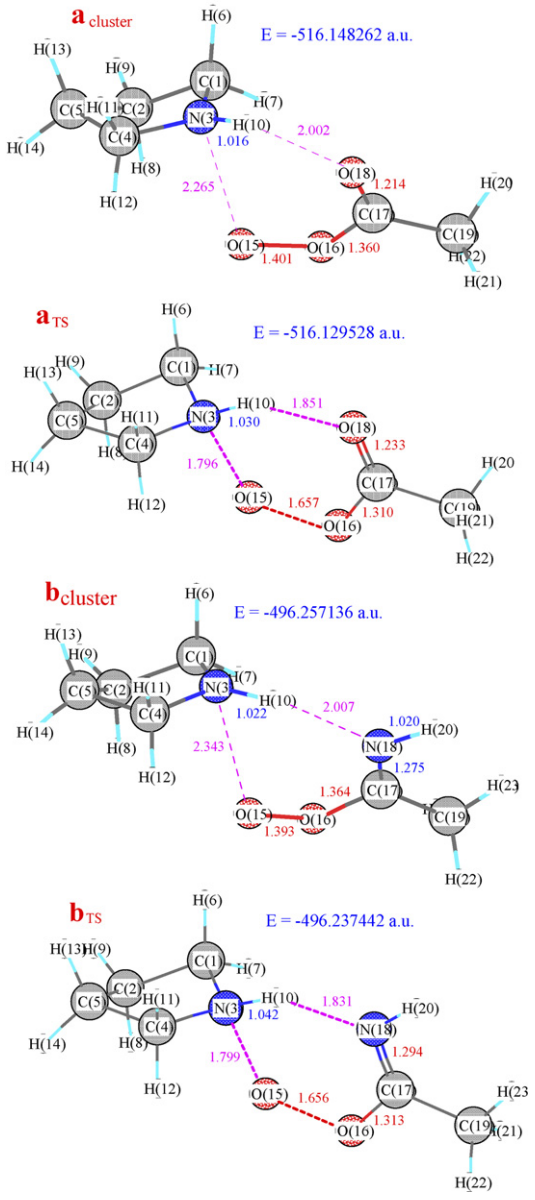

Fig. 5. Clusters $\mathbf{a}_{cluster}$ and $\mathbf{b}_{cluster}$ and transition structures $\mathbf{a}_{TS}$ and $\mathbf{b}_{TS}$ of oxidizing pyrrolidine by the peroxyl radicals of peracetic acid and percarboximidic acid obtained by calculation at the B3LYP/6-31G(d) level.

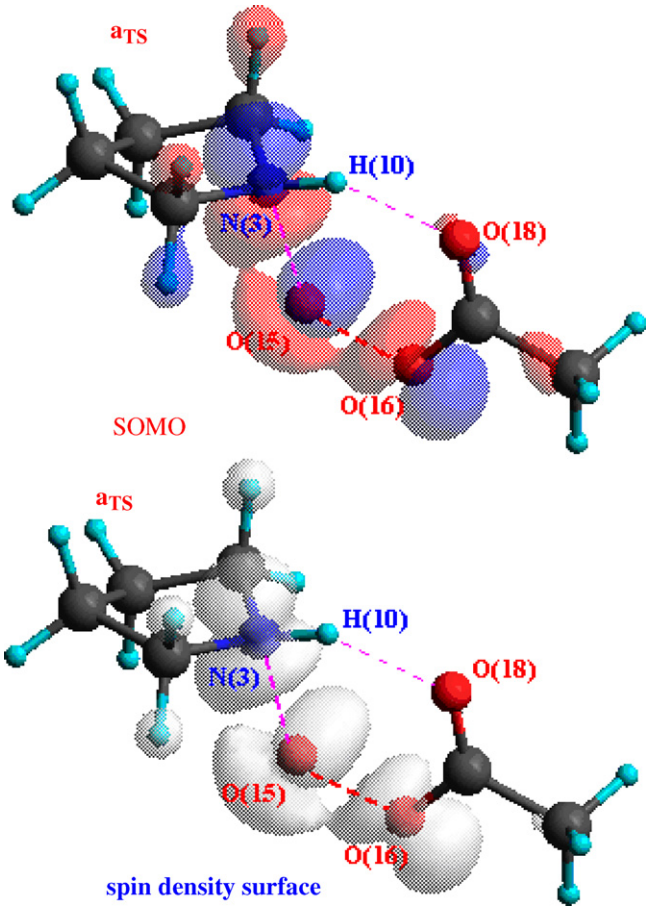

Fig. 6. SOMO graph (orbital contour value = 0.05) and spin density surface graph (isospin = 0.002) of transition structure ($\mathbf{a}_{TS}$) of pyrrolidine and the peroxyl radical of peracetic acid obtained by DFT calculation at the B3LYP/6-31G(d) level.

the influences of solvents CH_2Cl_2, CH_3CN and H_2O are shown in Table 5.

From the data in Table 5, the activation barriers (ΔE^*) calculated taking into account the influence of solvents were not significantly changed and they were 1–2 kcal/mol lower than the barriers (ΔE^*) in Table 4.

According to the above results and discussion, the mechanism for the formation of nitroxide radicals from secondary amine and peracid should be a peroxyl radical oxidation pathway. Taking the system of pyrrolidine and peracetic acid as an example, the mechanism for the formation of nitroxide radicals is as shown in Scheme 7.

The mechanism indicates that the formation of nitroxide radicals goes through three reaction steps (Scheme 7(**1**–**3**)).

Reaction 1 is the homolysis of the peroxy bond of peracids producing the two primary radicals. However, the activation barriers of this direct homolysis may be high. For the direct homolysis of the peroxy bond of aromatic peracids in Scheme 2(**1**), the authors [37,38] do not provide its activation barrier or rate constant. The process of production of primary radicals may not be as simple as reaction **1** in Scheme 2 or reaction **1** in Scheme 7. Some yeas ago Minisci and co-workers proposed a 'molecule-induced homolysis' process [47,48], which also produced two primary radicals. However,

Table 5
Activation barriers (ΔE^*) of pyrrolidine oxidation by peroxyl radicals of peracetic acid (**a**) or percarboximidic acid (**b**) based on electronic energies E_{TS}, $E_{cluster}$ obtained by using polarizable continuum model (PCM) at the B3LYP/6-31G(d) level

Solvent		E_{TS} (a.u.)	$E_{cluster}$ (a.u.)	ΔE^* (kcal/mol)
CH_2Cl_2	**a**	−516.135982	−516.152770	10.53
CH_2Cl_2	**b**	−496.244803	−496.262456	11.07
CH_3CN	**a**	−516.137066	−516.153582	10.36
CH_3CN	**b**	−496.246150	−496.263447	10.85
H_2O	**a**	−516.144807	−516.161052	10.19
H_2O	**b**	−496.255485	−496.272140	10.45

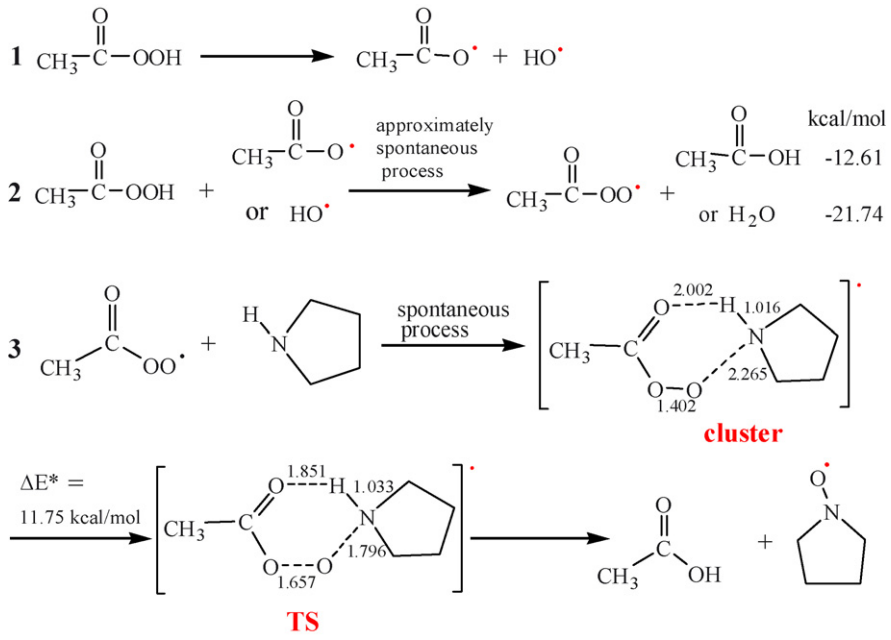

Scheme 7. The mechanism of forming its nitroxide radical of pyrrolidine by peracetic acid. The $\Delta E^{*} = 11.75$ kcal/mol in the scheme is the activation barrier of oxidizing pyrrolidine by the peroxyl radical of peracetic acid obtained by DFT calculation at the B3LYP/6-31G(d) level.

they do not provide the activation barrier or rate constant of the molecule-induced homolysis either. Therefore, how primary radicals are generated is a problem that chemists are still researching.

Reaction 2 is the generation of the peroxyl radical through hydrogen abstraction by the primary radicals. This is an approximately spontaneous process.

Reaction 3 is the oxidation of the secondary amine to the target nitroxide radical by the peroxyl radical, which is a process with low activation barrier. Reactions 2 and 3 indicated that once the primary radicals (Scheme 7(**1**)) form, both the generation of peroxyl radicals and the formation of the final nitroxide radical are very easy. Therefore, the rate-determining step in the peroxyl radical oxidation should be reaction **1** in Scheme 7, because the primary radicals are produced by the peroxy bond homolysis, which requires surmounting higher barriers than those in reactions **2** and **3**.

4.5. Microscopic view of nitroxide radical formation: a two-step process

The reason that the peroxyl radicals have high oxidation reactivity is that the terminal oxygen atom of the peroxyl radical can combine with the nitrogen atom of secondary amine and at the same time, the carbonyl or imido group of the peroxyl radicals can combine with the hydrogen atom on the nitrogen atom in secondary amines, which forms a good leaving group R–C(O)–OH (carboxylic acid) or R–C(O)–NH_2 (amide).

As an example, Fig. 7 shows the formation process of a nitroxide radical from pyrrolidine and the peroxyl radical of percarboximidic acid (system b). The IRC calculation at the B3LYP/6-31G(d) level revealed that the formation of the nitroxide radicals is a two-step process in which the terminal O(15) of the peroxyl radical is transferred to the N(3) of the secondary amine and an N–O bond forms first, then the H(10) of the secondary amine is transferred to the N(18) of the peroxyl radical. Finally, a nitroxide radical of pyrrolidine and an acetamide molecule are generated.

Table 6
The electron spin densities on N(3), O(15), and O(16) of the six structures in Fig. 7 and their energy changes (ΔE)

	N(3)	O(15)	O(16)	ΔE (kcal/mol)
$\mathbf{b}_{cluster}$	0.44	0.54	0.02	0
$\mathbf{b}_{TS}$	0.30	0.50	0.20	12.35
$\mathbf{b}_3$	0.04	0.52	0.44	−8.65
$\mathbf{b}_4$	0.02	0.60	0.37	−14.34
$\mathbf{b}_5$	0.08	0.76	0.14	−32.55
$\mathbf{b}_6$	0.45	0.55	0.00	−70.91

Something unusual was observed in the nitroxide radical formation process: from the cluster to $\mathbf{b}_4$, the spin density of the N atom of pyrrolidine was gradually decreased (Fig. 7($\mathbf{b}_{TS}$, $\mathbf{b}_3$ and $\mathbf{b}_4$)). After the $-NH_2$ group was generated by the hydrogen atom transfer, the spin density of the N atom of pyrrolidine rapidly increased again (Fig. 7($\mathbf{b}_5$)), and finally the unpaired electron completely belonged to the nitroxide radical (Fig. 7($\mathbf{b}_6$)).

The electron spin densities on N(3), O(15), and O(16) of the six structures in Fig. 7 and their energy changes are listed in Table 6. The data also indicated that the density on N(3) first decreases to approximately zero ($\mathbf{b}_3$ and $\mathbf{b}_4$) and then increases again as H(10) bonds to N(18) ($\mathbf{b}_5$). Finally, the unpaired electron entirely belongs to the nitroxide radical ($\mathbf{b}_6$). Another characteristic is that the energy of the final product system decreased by 70.91 kcal/mol, showing that the oxidation formed fairly stable radicals.

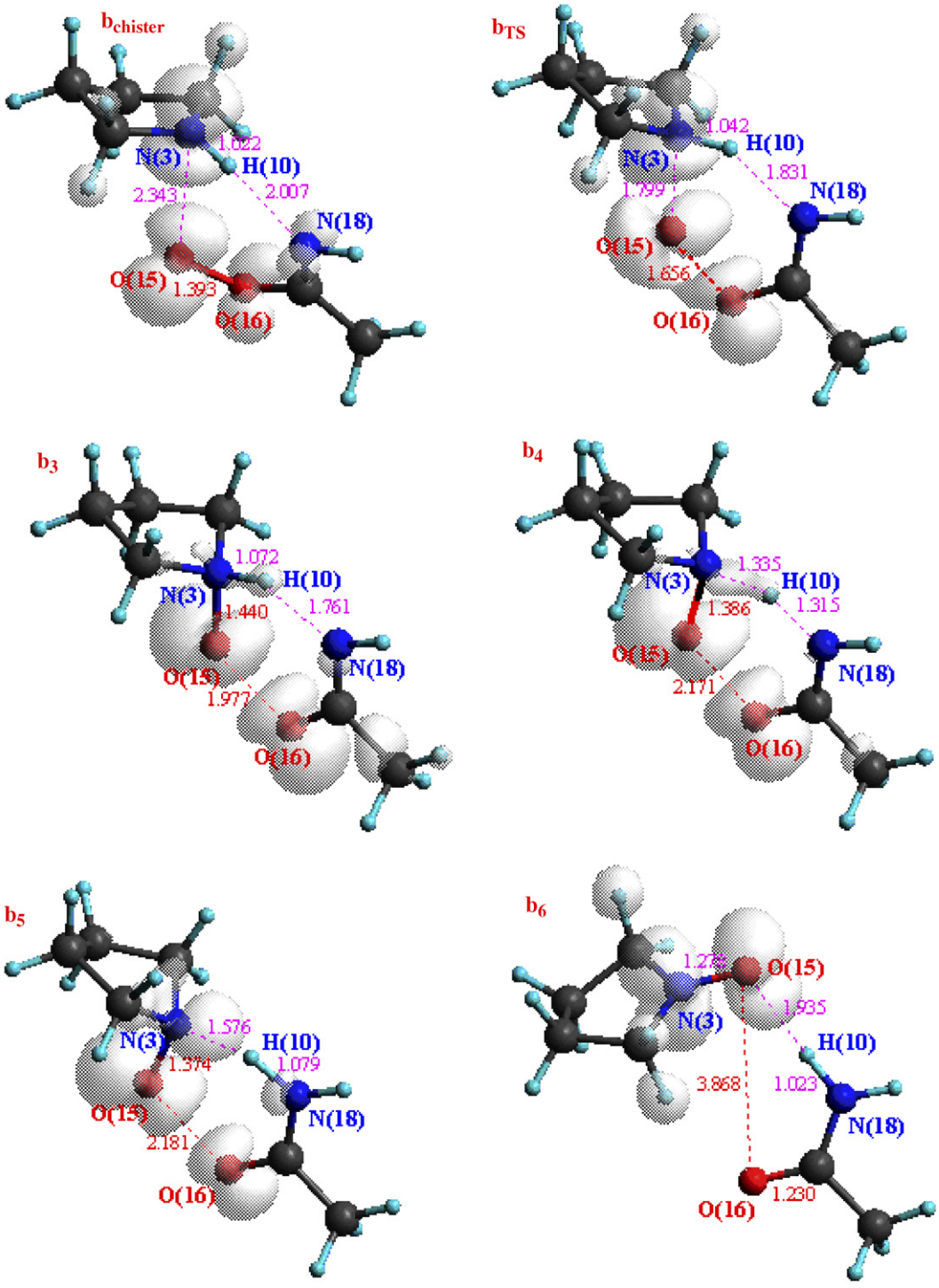

Fig. 7. Microscopic process from $\mathbf{b}_{cluster}$ to the nitroxide radical in the system of pyrrolidine and peroxyl radical $CH_3C(NH)OO^{\bullet}$ obtained by DFT calculation at the B3LYP/6-31G(d) level. Isospin = 0.002 a.u. The spin density surface graph $\mathbf{b}_{cluster}$ is from Opt calculation, $\mathbf{b}_3$, $\mathbf{b}_4$ and $\mathbf{b}_5$ are from IRC calculation and the graph $\mathbf{b}_6$ of final products is from IRC and Opt calculation.

5. Conclusions

In the present work based on ESR detection and DFT calculation, we reached the following conclusions.

1. In the preparation of nitroxide radicals by oxidation of secondary amines, the peroxyl radicals of peracids are reactive intermediates of the oxidant of the oxidation reaction.
2. The hydrogen abstraction by the primary radicals to form peroxyl radicals is an approximately spontaneous process.
3. The peroxyl radicals and secondary amines can spontaneously form clusters with energy reduction (~10 kcal/mol). In the clusters, about one-half of the unpaired electron

population of peroxyl radicals is already localized on the N atom of the secondary amine.

4. According to DFT calculation, the activation barriers of pyrrolidine oxidation by the peroxyl radicals of peracetic acid and peroxocarboximidic acid are only 11.75 and 12.35 kcal/mol, respectively. The barriers of the radical reactions are low. This means that the peroxyl radicals have high oxidation reactivity on secondary amines.
5. According to the above results the rate-determining step of the whole reaction should be the formation of the primary radicals through homolytic cleavage of the RO–OH bond of peracids. Once the primary radicals are formed, both the production of the peroxyl radicals and finally the formation of target nitroxide radicals are very easy.
6. The formation of nitroxide radicals is a two-step process of the terminal oxygen atom transfer of peroxyl radicals to the nitrogen atom of secondary amines followed by the hydrogen atom transfer from the N–H of secondary amines to the carbonyl oxygen atom or imido nitrogen atom of peracids.

Acknowledgments

We are grateful to the Institute of Medical Science, Tsinghua University, for their financial support of this research and to Professor Guoshi Wu, Institute of Physical Chemistry, Department of Chemistry, Tsinghua University, for their support and comments on quantum chemical calculation.

References

[1] R. Ziessel, C. Stroh, Synthesis 14 (2003) 2145.
[2] H. Kalman, H. Olga, Oxygen Radicals Scavengers Nat. Sci., Pap. Participants Congr. (1993) 63.
[3] M.J.T. Jean, Z.L. Guido, B. Mirna, R. Alessandra, Z. Martina, B.R. Francoise, C. Daniel, L. Patrick, G. Michel, Tetrahedron Lett. 32 (1991) 4129.
[4] S. Geneva, Helv. Chim. Acta 68 (1985) 1893.
[5] J.F.W. Keana, Chem. Rev. 78 (1977) 37.
[6] A.R. Forrester, J.M. Hay, R.H. Thomson, Organic Chemistry of Stable Radical, Academic Press, New York, 1976.
[7] E.G. Rozantsev, V.D. Scholle, Synthesis (1971) 190.
[8] M. Beyer, J. Fritscher, E. Feresin, O.J. Schiemann, Org. Chem. 68 (2003) 2209.
[9] J.F.W. Keana, Spin Labeling Theory and Application, vol. II, Academic Press, New York, 1979, Chapter 3.
[10] J.F.W. Keana, R.S. Norton, M. Morello, V. Engen, J. Clardy, J. Am. Chem. Soc. 100 (1978) 1618.
[11] B.J. Gaffney, in: L.J. Berliner (Ed.), Spin Labeling: Theory and Application, vol. I, Academic Press, New York, 1976 (Chapter 5).
[12] J.A. Cella, J.A. Kelley, E.F. Kenehan, Tetrahedron Lett. (1975) 2869.
[13] J.A. Cella, J.A. Kelley, E.F. Kenehan, J. Org. Chem. 40 (1975) 1860.
[14] B.J. Ganem, Org. Chem. 40 (1975) 1998.
[15] J.A. Cella, J.A. Kelley, E.F. Kenehan, J. Chem. Soc., Chem. Commun. (1974) 943.
[16] R. Ramasseul, A. Rassat, Tetrahedron Lett. (1971) 4623.
[17] E.G. Rozantsev, Free Nitroxyl Radical, Plenum Press, New York, 1970.
[18] J.F.W. Keana, S.B. Keana, D. Beetham, J. Am. Chem. Soc. 89 (1967) 3055.
[19] N. Peter, B. Lucienne, V.B. Martin, WO 2004,085,397 (2004).
[20] G. Jean-Philippe, G. Olivier, L. Jean-Pierre, (Fr.) WO 2000,040,550 (2000).
[21] G. Jean-Philippe, G. Olivier, T. Paul, (Fr.) WO 2000,040,526 (2000).
[22] G.B. Payne, D.M. Deming, D.H. Williams, J. Org. Chem. 40 (1961) 659.
[23] E.J. Rauckman, G.M. Rosen, M.B. Abou-Donia, Synth. Commun. 5 (1975) 409.
[24] M.J. Frisch, G.W. Trucks, H.B. Schlegel, G.E. Scuseria, M.A. Robb, J.R. Cheeseman, V.G. Zakrzewski, J.A. Montgomery Jr., R.E. Stratmann, J.C. Burant, S. Dapprich, J.M. Millam, A.D. Daniels, K.N. Kudin, M.C. Strain, O. Farkas, J. Tomasi, V. Barone, M. Cossi, R. Cammi, B. Mennucci, C. Pomelli, C. Adamo, S. Clifford, J. Ochterski, G.A. Petersson, P.Y. Ayala, Q. Cui, K. Morokuma, D.K. Malick, A.D. Rabuck, K. Raghavachari, J.B. Foresman, J. Cioslowski, J.V. Ortiz, A.G. Baboul, B.B. Stefanov, G. Liu, A. Liashenko, P. Piskorz, I. Komaromi, R. Gomperts, R.L. Martin, D.J. Fox, T. Keith, M.A. Al-Laham, C.Y. Peng, A. Nanayakkara, M. Challacombe, P.M.W. Gill, B. Johnson, W. Chen, M.W. Wong, J.L. Andres, C. Gonzalez, M. Head-Gordon, E.S. Replogle, J.A. Pople, Gaussian 98, Revision A.9, Gaussian, Inc., Pittsburgh, PA, 1998.
[25] D.V. Deubel, J. Sundermeyer, G.J. Frenking, J. Am. Chem. Soc. 122 (2000) 10101.
[26] D.V. Deubel, J. Sundermeyer, G. Frenking, Eur. J. Inorg. Chem. (2001) 1819.
[27] C.D. Valentin, P. Gisdakis, I.V. Yudanov, N.J. Rosch, Org. Chem. 65 (2000) 2996.
[28] R.D. Bach, C. Esteves, J.E. Winter, M.N. Glukhovtsev, J. Am. Chem. Soc. 120 (1998) 680.
[29] C. Kim, T.G. Traylor, C.L. Perrin, J. Am. Chem. Soc. 120 (1998) 9513.
[30] M. Freccero, R. Gandolfi, M. Sarzi-Amade, A. Rastelli, J. Org. Chem. 65 (2000) 8948.
[31] M. Freccero, R. Gandolfi, M. Sarzi-Amade, A. Rastelli, J. Org. Chem. 65 (2000) 2030.
[32] M. Cossi, V. Barone, B. Mennucci, J. Tomasi, Chem. Phys. Lett. 286 (1998) 253.
[33] V. Barone, M. Cossi, J. Tomasi, J. Comp. Chem. 19 (1998) 404.
[34] V. Barone, M. Cossi, J. Phys. Chem. A 102 (1998) 1995.
[35] B. Mennucci, R. Cammi, J. Tomasi, J. Chem. Phys. 109 (1998) 2798.
[36] R. Briere, A. Rassat, Tetrahedron 32 (1976) 2891.
[37] J. Fossey, D. Lefort, J. Sorba, Radical in Organic Chemistry, Wiley, New York, 1995, p. 217.
[38] K. Tokumaru, O. Simamura, Bull. Chem. Soc. Jpn. 35 (1962) 1679.
[39] F. Minisci, F. Fontana, S. Araneo, F. Recupero, S. Banfi, S. Quici, J. Am. Chem. Soc. 117 (1995) 226.
[40] B. Meunier, Chem. Rev. 92 (1992) 1411.
[41] A. Bravo, H.R. Bjorsvik, F. Fontana, F. Minisci, A. Serri, J. Org. Chem. 61 (1996) 9409.
[42] J. Chateauneuf, J. Lusztyk, K.U. Ingold, J. Am. Chem. Soc. 109 (1987) 897.
[43] J. Chateauneuf, J. Lusztyk, K.U. Ingold, J. Am. Chem. Soc. 110 (1988) 2877–2886.
[44] K.B. Wiberg, J. Am. Chem. Soc. 75 (1953) 3961.
[45] K.B. Wiberg, J. Am. Chem. Soc. 77 (1955) 2519.
[46] J.E. McIsaac Jr., R.E. Ball, E.J. Behrman, J. Org. Chem. 36 (1971) 3048.
[47] A. Bravo, F. Fontana, G. Fronza, F. Minisci, L. Zhao, J. Org. Chem. 63 (1998) 254.
[48] F. Minisci, C. Gambarotti, M. Pierini, O. Porta, C. Punta, F. Recupero, M. Lucarinib, V. Mugnain, Tetrahedron Lett. 47 (2006) 1421.